

Graph Regularized Non-negative Matrix Factorization for Data Representation

Deng Cai, *Member, IEEE*, Xiaofei He, *Senior Member, IEEE*, Jiawei Han, *Fellow, IEEE*
Thomas S. Huang, *Life Fellow, IEEE*

Abstract—Matrix factorization techniques have been frequently applied in information retrieval, computer vision and pattern recognition. Among them, Non-negative Matrix Factorization (NMF) has received considerable attention due to its psychological and physiological interpretation of naturally occurring data whose representation may be parts-based in the human brain. On the other hand, from the geometric perspective, the data is usually sampled from a low dimensional manifold embedded in a high dimensional ambient space. One hopes then to find a compact representation which uncovers the hidden semantics and simultaneously respects the intrinsic geometric structure. In this paper, we propose a novel algorithm, called *Graph Regularized Non-negative Matrix Factorization* (GNMF), for this purpose. In GNMF, an affinity graph is constructed to encode the geometrical information, and we seek a matrix factorization which respects the graph structure. Our empirical study shows encouraging results of the proposed algorithm in comparison to the state-of-the-art algorithms on real world problems.

Index Terms—Non-negative Matrix Factorization, Graph Laplacian, Manifold Regularization, Clustering.



1 INTRODUCTION

The techniques for matrix factorization have become popular in recent years for data representation. In many problems in information retrieval, computer vision and pattern recognition, the input data matrix is of very high dimension. This makes *learning from example* infeasible [15]. One hopes then to find two or more lower dimensional matrices whose product provides a good approximation to the original one. The canonical matrix factorization techniques include LU-decomposition, QR-decomposition, Vector Quantization, and Singular Value Decomposition (SVD).

SVD is one of the most frequently used matrix factorization techniques. A **singular value decomposition** of an $M \times N$ matrix \mathbf{X} has the following form:

$$\mathbf{X} = \mathbf{U}\mathbf{\Sigma}\mathbf{V}^T,$$

where \mathbf{U} is an $M \times M$ **orthogonal matrix**, \mathbf{V} is an $N \times N$ orthogonal matrix, and $\mathbf{\Sigma}$ is an $M \times N$ diagonal matrix with $\Sigma_{ij} = 0$ if $i \neq j$ and $\Sigma_{ii} \geq 0$. The quantities Σ_{ii} are called the *singular values* of \mathbf{X} , and the columns of \mathbf{U} and \mathbf{V} are called left and right *singular vectors*, respectively. By removing those singular vectors corresponding to

sufficiently small singular values, we get a low-rank approximation to the original matrix. This approximation is optimal in terms of the reconstruction error and thus optimal for data representation when Euclidean structure is concerned. For this reason, SVD has been applied to various real world applications, such as face recognition (*Eigenface*, [40]) and document representation (*Latent Semantic Indexing*, [11]).

Previous studies have shown that there is psychological and physiological evidence for parts-based representation in the human brain [34], [41], [31]. The Non-negative Matrix Factorization (NMF) algorithm is proposed to learn the parts of objects like human faces and text documents [33], [26]. NMF aims to find two non-negative matrices whose product provides a good approximation to the original matrix. The non-negative constraints lead to a parts-based representation because they allow only additive, not subtractive, combinations. NMF has been shown to be superior to SVD in face recognition [29] and document clustering [42]. It is optimal for learning the parts of objects.

Recently, various researchers (see [39], [35], [1], [36], [2]) have considered the case when the data is drawn from sampling a probability distribution that has support on or near to a *submanifold* of the ambient space. Here, a d -dimensional submanifold of a Euclidean space \mathbb{R}^M is a subset $\mathcal{M}^d \subset \mathbb{R}^M$ which locally looks like a flat d -dimensional Euclidean space [28]. In order to detect the underlying manifold structure, many *manifold learning* algorithms have been proposed, such as Locally Linear Embedding (LLE) [35], ISOMAP [39], and Laplacian Eigenmap [1]. All these algorithms use the so-called locally invariant idea [18], *i.e.*, the nearby points are

D. Cai and X. He are with the State Key Lab of CAD&CG, College of Computer Science, Zhejiang University, Hangzhou, Zhejiang, China, 310058. Email: {dengcai, xiaofeihe}@cad.zju.edu.cn.

J. Han is with the Department of Computer Science, University of Illinois at Urbana Champaign, 201 N. Goodwin Ave., Urbana, IL 61801. Email: hanj@cs.uiuc.edu.

T. Huang is with the Beckman Institute for Advanced Sciences and Technology, University of Illinois at Urbana Champaign, 405 North Mathews Ave., Urbana, IL 61801. Email: huang@ifp.uiuc.edu.

Manuscript received 28 Apr. 2009; revised 21 Dec. 2009; accepted 22 Oct. 2010

likely to have similar embeddings. It has been shown that learning performance can be significantly enhanced if the geometrical structure is exploited and the local invariance is considered.

Motivated by recent progress in matrix factorization and manifold learning [2], [5], [6], [7], in this paper we propose a novel algorithm, called Graph regularized Non-negative Matrix Factorization (GNMF), which explicitly considers the local invariance. We encode the geometrical information of the data space by constructing a nearest neighbor graph. Our goal is to find a parts-based representation space in which two data points are sufficiently close to each other if they are connected in the graph. To achieve this, we design a new matrix factorization objective function and incorporate the graph structure into it. We also develop an optimization scheme to solve the objective function based on iterative updates of the two factor matrices. This leads to a new parts-based data representation which respects the geometrical structure of the data space. The convergence proof of our optimization scheme is provided.

It is worthwhile to highlight several aspects of the proposed approach here:

- 1) While the standard NMF fits the data in a Euclidean space, our algorithm exploits the intrinsic geometry of the data distribution and incorporates it as an additional regularization term. Hence, our algorithm is particularly applicable when the data is sampled from a submanifold which is embedded in high dimensional ambient space.
- 2) Our algorithm constructs a nearest neighbor graph to model the manifold structure. The weight matrix of the graph is highly sparse. Therefore, the multiplicative update rules for GNMF are very efficient. By preserving the graph structure, our algorithm can have more discriminating power than the standard NMF algorithm.
- 3) Recent studies [17], [13] show that NMF is closely related to Probabilistic Latent Semantic Analysis (PLSA) [21]. The latter is one of the most popular topic modeling algorithms. Specifically, NMF with KL-divergence formulation is equivalent to PLSA [13]. From this viewpoint, the proposed GNMF approach also provides a principled way for incorporating the geometrical structure into topic modeling.
- 4) The proposed framework is a general one that can leverage the power of both NMF and graph Laplacian regularization. Besides the nearest neighbor information, other knowledge (e.g., label information, social network structure) about the data can also be used to construct the graph. This naturally leads to other extensions (e.g., semi-supervised NMF).

The rest of the paper is organized as follows: in Section 2, we give a brief review of NMF. Section 3 introduces our algorithm and provides a convergence proof of our optimization scheme. Extensive experimental results on clustering are presented in Section 4. Finally, we provide

some concluding remarks and suggestions for future work in Section 5.

2 A BRIEF REVIEW OF NMF

Non-negative Matrix Factorization (NMF) [26] is a matrix factorization algorithm that focuses on the analysis of data matrices whose elements are nonnegative.

Given a data matrix $\mathbf{X} = [\mathbf{x}_1, \dots, \mathbf{x}_N] \in \mathbb{R}^{M \times N}$, each column of \mathbf{X} is a sample vector. NMF aims to find two non-negative matrices $\mathbf{U} = [u_{ik}] \in \mathbb{R}^{M \times K}$ and $\mathbf{V} = [v_{jk}] \in \mathbb{R}^{N \times K}$ whose product can well approximate the original matrix \mathbf{X} .

$$\mathbf{X} \approx \mathbf{U}\mathbf{V}^T.$$

There are two commonly used cost functions that quantifies the quality of the approximation. The first one is the square of the Euclidean distance between two matrices (the square of the *Frobenius norm* of two matrices difference) [33]:

$$O_1 = \|\mathbf{X} - \mathbf{U}\mathbf{V}^T\|^2 = \sum_{i,j} \left(x_{ij} - \sum_{k=1}^K u_{ik}v_{jk} \right)^2. \quad (1)$$

The second one is the “divergence” between two matrices [27]:

$$O_2 = D(\mathbf{X}||\mathbf{Y}) = \sum_{i,j} \left(x_{ij} \log \frac{x_{ij}}{y_{ij}} - x_{ij} + y_{ij} \right) \quad (2)$$

where $\mathbf{Y} = [y_{ij}] = \mathbf{U}\mathbf{V}^T$. This cost function is referred to as “divergence” of \mathbf{X} from \mathbf{Y} instead of “distance” between \mathbf{X} and \mathbf{Y} because it is not symmetric. In other words, $D(\mathbf{X}||\mathbf{Y}) \neq D(\mathbf{Y}||\mathbf{X})$. It reduces to the Kullback-Leibler divergence, or relative entropy, when $\sum_{i,j} x_{ij} = \sum_{i,j} y_{ij} = 1$, so that \mathbf{X} and \mathbf{Y} can be regarded as normalized probability distributions. We will refer O_1 as F-norm formulation and O_2 as divergence formulation in the rest of the paper.

Although the objective function O_1 in Eq. (1) and O_2 in Eq. (2) are convex in \mathbf{U} only or \mathbf{V} only, they are not convex in both variables together. Therefore it is unrealistic to expect an algorithm to find the global minimum of O_1 (or, O_2). Lee & Seung [27] presented two iterative update algorithms. The algorithm minimizing the objective function O_1 in Eq. (1) is as follows:

$$u_{ik} \leftarrow u_{ik} \frac{(\mathbf{X}\mathbf{V})_{ik}}{(\mathbf{U}\mathbf{V}^T\mathbf{V})_{ik}}, \quad v_{jk} \leftarrow v_{jk} \frac{(\mathbf{X}^T\mathbf{U})_{jk}}{(\mathbf{V}\mathbf{U}^T\mathbf{U})_{jk}}$$

The algorithm minimizing the objective function O_2 in Eq. (2) is:

$$u_{ik} \leftarrow u_{ik} \frac{\sum_j (x_{ij}v_{jk} / \sum_k u_{ik}v_{jk})}{\sum_j v_{jk}}, \quad v_{jk} \leftarrow v_{jk} \frac{\sum_i (x_{ij}u_{ik} / \sum_k u_{ik}v_{jk})}{\sum_i u_{ik}}$$

It is proved that the above two algorithms will find local minima of the objective functions O_1 and O_2 [27].

In reality, we have $K \ll M$ and $K \ll N$. Thus, NMF essentially tries to find a compressed approximation of the original data matrix. We can view this approximation column by column as

$$\mathbf{x}_j \approx \sum_{k=1}^K \mathbf{u}_k v_{jk} \quad (3)$$

where \mathbf{u}_k is the k -th column vector of \mathbf{U} . Thus, each data vector \mathbf{x}_j is approximated by a linear combination of the columns of \mathbf{U} , weighted by the components of \mathbf{V} . Therefore \mathbf{U} can be regarded as containing a basis that is optimized for the linear approximation of the data in \mathbf{X} . Let \mathbf{z}_j^T denote the j -th row of \mathbf{V} , $\mathbf{z}_j = [v_{j1}, \dots, v_{jk}]^T$. \mathbf{z}_j can be regarded as the new representation of the j -th data point with respect to the new basis \mathbf{U} . Since relatively few basis vectors are used to represent many data vectors, a good approximation can only be achieved if the basis vectors discover structure that is latent in the data [27].

The non-negative constraints on \mathbf{U} and \mathbf{V} only allow additive combinations among different bases. This is the most significant difference between NMF and the other matrix factorization methods, e.g., SVD. Unlike SVD, no subtractions can occur in NMF. For this reason, it is believed that NMF can learn a *parts-based* representation [26]. The advantages of this parts-based representation have been observed in many real world problems such as face analysis [29], document clustering [42] and DNA gene expression analysis [3].

3 GRAPH REGULARIZED NON-NEGATIVE MATRIX FACTORIZATION

By using the non-negative constraints, NMF can learn a parts-based representation. However, NMF performs this learning in the Euclidean space. It fails to discover the intrinsic geometrical and discriminating structure of the data space, which is essential to the real-world applications. In this section, we introduce our *Graph regularized Non-negative Matrix Factorization* (GNMF) algorithm which avoids this limitation by incorporating a geometrically based regularizer.

3.1 NMF with Manifold Regularization

Recall that NMF tries to find a set of basis vectors that can be used to best approximate the data. One might further hope that the basis vectors can respect the intrinsic Riemannian structure, rather than ambient Euclidean structure. A natural assumption here could be that if two data points $\mathbf{x}_j, \mathbf{x}_l$ are close in the intrinsic geometry of the data distribution, then \mathbf{z}_j and \mathbf{z}_l , the representations of this two points with respect to the new basis, are also close to each other. This assumption is usually referred to as *local invariance assumption* [1], [19], [7], which plays an essential role in the development of various kinds of algorithms including dimensionality

reduction algorithms [1] and semi-supervised learning algorithms [2], [46], [45].

Recent studies in spectral graph theory [9] and manifold learning theory [1] have demonstrated that the local geometric structure can be effectively modeled through a nearest neighbor graph on a scatter of data points. Consider a graph with N vertices where each vertex corresponds to a data point. For each data point \mathbf{x}_j , we find its p nearest neighbors and put edges between \mathbf{x}_j and its neighbors. There are many choices to define the weight matrix \mathbf{W} on the graph. Three of the most commonly used are as follows:

- 1) **0-1 weighting.** $\mathbf{W}_{jl} = 1$ if and only if nodes j and l are connected by an edge. This is the simplest weighting method and is very easy to compute.
- 2) **Heat kernel weighting.** If nodes j and l are connected, put

$$\mathbf{W}_{jl} = e^{-\frac{\|\mathbf{x}_j - \mathbf{x}_l\|^2}{\sigma}}$$

Heat kernel has an intrinsic connection to the Laplace Beltrami operator on differentiable functions on a manifold [1].

- 3) **Dot-product weighting.** If nodes j and l are connected, put

$$\mathbf{W}_{jl} = \mathbf{x}_j^T \mathbf{x}_l$$

Note that, if \mathbf{x} is normalized to 1, the dot product of two vectors is equivalent to the cosine similarity of the two vectors.

The \mathbf{W}_{jl} is used to measure the closeness of two points \mathbf{x}_j and \mathbf{x}_l . The different similarity measures are suitable for different situations. For example, the cosine similarity (Dot-product weighting) is very popular in the IR community (for processing documents). While for image data, the heat kernel weight may be a better choice. Since \mathbf{W}_{jl} in our paper is only for measuring the closeness, we do not treat the different weighting schemes separately.

The low dimensional representation of \mathbf{x}_j with respect to the new basis is $\mathbf{z}_j = [v_{j1}, \dots, v_{jk}]^T$. Again, we can use either Euclidean distance

$$d(\mathbf{z}_j, \mathbf{z}_l) = \|\mathbf{z}_j - \mathbf{z}_l\|^2$$

or divergence

$$D(\mathbf{z}_j || \mathbf{z}_l) = \sum_{k=1}^K \left(v_{jk} \log \frac{v_{jk}}{v_{lk}} - v_{jk} + v_{lk} \right),$$

to measure the “dissimilarity” between the low dimensional representations of two data points with respect to the new basis.

With the above defined weight matrix \mathbf{W} , we can use the following two terms to measure the smoothness of the low dimensional representation.

$$\begin{aligned} \mathcal{R}_2 &= \frac{1}{2} \sum_{j,l=1}^N \left(D(\mathbf{z}_j || \mathbf{z}_l) + D(\mathbf{z}_l || \mathbf{z}_j) \right) \mathbf{W}_{jl} \\ &= \frac{1}{2} \sum_{j,l=1}^N \sum_{k=1}^K \left(v_{jk} \log \frac{v_{jk}}{v_{lk}} + v_{lk} \log \frac{v_{lk}}{v_{jk}} \right) \mathbf{W}_{jl}. \end{aligned} \quad (4)$$

and

$$\begin{aligned}\mathcal{R}_1 &= \frac{1}{2} \sum_{j,l=1}^N \|\mathbf{z}_j - \mathbf{z}_l\|^2 \mathbf{W}_{jl} \\ &= \sum_{j=1}^N \mathbf{z}_j^T \mathbf{z}_j \mathbf{D}_{jj} - \sum_{j,l=1}^N \mathbf{z}_j^T \mathbf{z}_l \mathbf{W}_{jl} \\ &= \text{Tr}(\mathbf{V}^T \mathbf{D} \mathbf{V}) - \text{Tr}(\mathbf{V}^T \mathbf{W} \mathbf{V}) = \text{Tr}(\mathbf{V}^T \mathbf{L} \mathbf{V}),\end{aligned}\quad (5)$$

where $\text{Tr}(\cdot)$ denotes the trace of a matrix and \mathbf{D} is a diagonal matrix whose entries are column (or row, since \mathbf{W} is symmetric) sums of \mathbf{W} , $\mathbf{D}_{jj} = \sum_l \mathbf{W}_{jl}$. $\mathbf{L} = \mathbf{D} - \mathbf{W}$, which is called graph Laplacian [9].

By minimizing \mathcal{R}_1 (or, \mathcal{R}_2), we expect that if two data points \mathbf{x}_j and \mathbf{x}_l are close (*i.e.* \mathbf{W}_{jl} is big), \mathbf{z}_j and \mathbf{z}_l are also close to each other. Combining this geometrically based regularizer with the original NMF objective function leads to our Graph regularized Non-negative Matrix Factorization (GNMF).

Given a data matrix $\mathbf{X} = [x_{ij}] \in \mathbb{R}^{M \times N}$, Our GNMF aims to find two non-negative matrices $\mathbf{U} = [u_{ik}] \in \mathbb{R}^{M \times K}$ and $\mathbf{V} = [v_{jk}] \in \mathbb{R}^{N \times K}$. Similar to NMF, we can also use two “distance” measures here. If the Euclidean distance is used, GNMF minimizes the objective function as follows:

$$\mathcal{O}_1 = \|\mathbf{X} - \mathbf{UV}^T\|^2 + \lambda \text{Tr}(\mathbf{V}^T \mathbf{L} \mathbf{V}). \quad (6)$$

If the divergence is used, GNMF minimizes

$$\begin{aligned}\mathcal{O}_2 &= \sum_{i=1}^M \sum_{j=1}^N \left(x_{ij} \log \frac{x_{ij}}{\sum_{k=1}^K u_{ik} v_{jk}} - x_{ij} + \sum_{k=1}^K u_{ik} v_{jk} \right) \\ &\quad + \frac{\lambda}{2} \sum_{j=1}^N \sum_{l=1}^N \sum_{k=1}^K \left(v_{jk} \log \frac{v_{jk}}{v_{lk}} + v_{lk} \log \frac{v_{lk}}{v_{jk}} \right) \mathbf{W}_{jl}\end{aligned}\quad (7)$$

Where the regularization parameter $\lambda \geq 0$ controls the smoothness of the new representation.

3.2 Updating Rules Minimizing Eq. (6)

The objective function \mathcal{O}_1 and \mathcal{O}_2 of GNMF in Eq. (6) and Eq. (7) are not convex in both \mathbf{U} and \mathbf{V} together. Therefore it is unrealistic to expect an algorithm to find the global minima. In the following, we introduce two iterative algorithms which can achieve local minima.

We first discuss how to minimize the objective function \mathcal{O}_1 , which can be rewritten as:

$$\begin{aligned}\mathcal{O}_1 &= \text{Tr}((\mathbf{X} - \mathbf{UV}^T)(\mathbf{X} - \mathbf{UV}^T)^T) + \lambda \text{Tr}(\mathbf{V}^T \mathbf{L} \mathbf{V}) \\ &= \text{Tr}(\mathbf{X} \mathbf{X}^T) - 2 \text{Tr}(\mathbf{X} \mathbf{V} \mathbf{U}^T) + \text{Tr}(\mathbf{U} \mathbf{V}^T \mathbf{V} \mathbf{U}^T) \\ &\quad + \lambda \text{Tr}(\mathbf{V}^T \mathbf{L} \mathbf{V})\end{aligned}\quad (8)$$

where the second equality applies the matrix properties $\text{Tr}(\mathbf{AB}) = \text{Tr}(\mathbf{BA})$ and $\text{Tr}(\mathbf{A}) = \text{Tr}(\mathbf{A}^T)$. Let ψ_{ik} and ϕ_{jk} be the Lagrange multiplier for constraint $u_{ik} \geq 0$ and $v_{jk} \geq 0$ respectively, and $\Psi = [\psi_{ik}]$, $\Phi = [\phi_{jk}]$, the Lagrange \mathcal{L} is

$$\begin{aligned}\mathcal{L} &= \text{Tr}(\mathbf{X} \mathbf{X}^T) - 2 \text{Tr}(\mathbf{X} \mathbf{V} \mathbf{U}^T) + \text{Tr}(\mathbf{U} \mathbf{V}^T \mathbf{V} \mathbf{U}^T) \\ &\quad + \lambda \text{Tr}(\mathbf{V}^T \mathbf{L} \mathbf{V}) + \text{Tr}(\Psi \mathbf{U}^T) + \text{Tr}(\Phi \mathbf{V}^T)\end{aligned}\quad (9)$$

The partial derivatives of \mathcal{L} with respect to \mathbf{U} and \mathbf{V} are:

$$\frac{\partial \mathcal{L}}{\partial \mathbf{U}} = -2\mathbf{X} \mathbf{V} + 2\mathbf{U} \mathbf{V}^T \mathbf{V} + \Psi \quad (10)$$

$$\frac{\partial \mathcal{L}}{\partial \mathbf{V}} = -2\mathbf{X}^T \mathbf{U} + 2\mathbf{V} \mathbf{U}^T \mathbf{U} + 2\lambda \mathbf{L} \mathbf{V} + \Phi \quad (11)$$

Using the KKT conditions $\psi_{ik} u_{ik} = 0$ and $\phi_{jk} v_{jk} = 0$, we get the following equations for u_{ik} and v_{jk} :

$$-(\mathbf{X} \mathbf{V})_{ik} u_{ik} + (\mathbf{U} \mathbf{V}^T \mathbf{V})_{ik} u_{ik} = 0 \quad (12)$$

$$-(\mathbf{X}^T \mathbf{U})_{jk} v_{jk} + (\mathbf{V} \mathbf{U}^T \mathbf{U})_{jk} v_{jk} + \lambda (\mathbf{L} \mathbf{V})_{jk} v_{jk} = 0 \quad (13)$$

These equations lead to the following updating rules:

$$u_{ik} \leftarrow u_{ik} \frac{(\mathbf{X} \mathbf{V})_{ik}}{(\mathbf{U} \mathbf{V}^T \mathbf{V})_{ik}} \quad (14)$$

$$v_{jk} \leftarrow v_{jk} \frac{(\mathbf{X}^T \mathbf{U} + \lambda \mathbf{W} \mathbf{V})_{jk}}{(\mathbf{V} \mathbf{U}^T \mathbf{U} + \lambda \mathbf{D} \mathbf{V})_{jk}} \quad (15)$$

Regarding these two updating rules, we have the following theorem:

Theorem 1: The objective function \mathcal{O}_1 in Eq. (6) is nonincreasing under the updating rules in Eq. (14) and (15).

Please see the Appendix for a detailed proof for the above theorem. Our proof essentially follows the idea in the proof of Lee and Seung’s paper [27] for the original NMF. Recent studies [8], [30] show that Lee and Seung’s multiplicative algorithm [27] cannot guarantee the convergence to a stationary point. Particularly, Lin [30] suggests minor modifications on Lee and Seung’s algorithm which can converge. Our updating rules in Eq. (14) and (15) are essentially similar to the updating rules for NMF and therefore Lin’s modifications can also be applied.

When $\lambda = 0$, it is easy to check that the updating rules in Eq. (14) and (15) reduce to the updating rules of the original NMF.

For the objective function of NMF, it is easy to check that if \mathbf{U} and \mathbf{V} are the solution, then, $\mathbf{U} \mathbf{D}$, $\mathbf{V} \mathbf{D}^{-1}$ will also form a solution for any positive diagonal matrix \mathbf{D} . To eliminate this uncertainty, in practice people will further require that the Euclidean length of each column vector in matrix \mathbf{U} (or \mathbf{V}) is 1 [42]. The matrix \mathbf{V} (or \mathbf{U}) will be adjusted accordingly so that $\mathbf{U} \mathbf{V}^T$ does not change. This can be achieved by:

$$u_{ik} \leftarrow \frac{u_{ik}}{\sqrt{\sum_i u_{ik}^2}}, \quad v_{jk} \leftarrow v_{jk} \sqrt{\sum_i u_{ik}^2} \quad (16)$$

Our GNMF also adopts this strategy. After the multiplicative updating procedure converges, we set the Euclidean length of each column vector in matrix \mathbf{U} to 1 and adjust the matrix \mathbf{V} so that $\mathbf{U} \mathbf{V}^T$ does not change.

3.3 Connection to Gradient Descent Method

Another general algorithm for minimizing the objective function of GNMF in Eq. (6) is gradient descent [25]. For our problem, gradient descent leads to the following additive update rules:

$$u_{ik} \leftarrow u_{ik} + \eta_{ik} \frac{\partial \mathcal{O}_1}{\partial u_{ik}}, \quad v_{jk} \leftarrow v_{jk} + \delta_{jk} \frac{\partial \mathcal{O}_1}{\partial v_{jk}} \quad (17)$$

The η_{ik} and δ_{jk} are usually referred as step size parameters. As long as η_{ik} and δ_{jk} are sufficiently small, the above updates should reduce \mathcal{O}_1 unless \mathbf{U} and \mathbf{V} are at a stationary point.

Generally speaking, it is relatively difficult to set these step size parameters while still maintaining the non-negativity of u_{ik} and v_{jk} . However, with the special form of the partial derivatives, we can use some tricks to set the step size parameters automatically. Let $\eta_{ik} = -u_{ik}/2(\mathbf{UV}^T\mathbf{V})_{ik}$, we have

$$\begin{aligned} u_{ik} + \eta_{ik} \frac{\partial \mathcal{O}_1}{\partial u_{ik}} &= u_{ik} - \frac{u_{ik}}{2(\mathbf{UV}^T\mathbf{V})_{ik}} \frac{\partial \mathcal{O}_1}{\partial u_{ik}} \\ &= u_{ik} - \frac{u_{ik}}{2(\mathbf{UV}^T\mathbf{V})_{ik}} \left(-2(\mathbf{XV})_{ik} + 2(\mathbf{UV}^T\mathbf{V})_{ik} \right) \\ &= u_{ik} \frac{(\mathbf{XV})_{ik}}{(\mathbf{UV}^T\mathbf{V})_{ik}} \end{aligned} \quad (18)$$

Similarly, let $\delta_{jk} = -v_{jk}/2(\mathbf{VU}^T\mathbf{U} + \lambda\mathbf{DV})_{jk}$, we have

$$\begin{aligned} v_{jk} + \delta_{jk} \frac{\partial \mathcal{O}_1}{\partial v_{jk}} &= v_{jk} - \frac{v_{jk}}{2(\mathbf{VU}^T\mathbf{U} + \lambda\mathbf{DV})_{jk}} \frac{\partial \mathcal{O}_1}{\partial v_{jk}} \\ &= v_{jk} - \frac{v_{jk}}{2(\mathbf{VU}^T\mathbf{U} + \lambda\mathbf{DV})_{jk}} \left(-2(\mathbf{X}^T\mathbf{U})_{jk} \right. \\ &\quad \left. + 2(\mathbf{VU}^T\mathbf{U})_{jk} + 2\lambda(\mathbf{LV})_{jk} \right) \\ &= v_{jk} \frac{(\mathbf{X}^T\mathbf{U} + \lambda\mathbf{WV})_{jk}}{(\mathbf{VU}^T\mathbf{U} + \lambda\mathbf{DV})_{jk}} \end{aligned} \quad (19)$$

Now it is clear that the multiplicative updating rules in Eq. (14) and Eq. (15) are special cases of gradient descent with an automatic step parameter selection. The advantage of multiplicative updating rules is the guarantee of non-negativity of \mathbf{U} and \mathbf{V} . Theorem 1 also guarantees that the multiplicative updating rules in Eq. (14) and (15) converge to a local optimum.

3.4 Updating Rules Minimizing Eq. (7)

For the divergence formulation of GNMF, we also have two updating rules which can achieve a local minimum of Eq. (7).

$$u_{ik} \leftarrow u_{ik} \frac{\sum_j (x_{ij}v_{jk} / \sum_k u_{ik}v_{jk})}{\sum_j v_{jk}} \quad (20)$$

$$\mathbf{v}_k \leftarrow \left(\sum_i u_{ik} \mathbf{I} + \lambda \mathbf{L} \right)^{-1} \begin{bmatrix} v_{1k} \sum_i \left(x_{i1}u_{ik} / \sum_k u_{ik}v_{1k} \right) \\ v_{2k} \sum_i \left(x_{i2}u_{ik} / \sum_k u_{ik}v_{2k} \right) \\ \vdots \\ v_{Nk} \sum_i \left(x_{iN}u_{ik} / \sum_k u_{ik}v_{Nk} \right) \end{bmatrix}, \quad (21)$$

where \mathbf{v}_k is the k -th column of \mathbf{V} and \mathbf{I} is an $N \times N$ identity matrix.

Similarly, we have the following theorem:

Theorem 2: The objective function \mathcal{O}_2 in Eq. (7) is non-increasing with the updating rules in Eq. (20) and (21). The objective function is invariant under these updates if and only if \mathbf{U} and \mathbf{V} are at a stationary point.

Please see the Appendix for a detailed proof. The updating rules in this subsection (minimizing the divergence formulation of Eq. (7)) are different from the updating rules in Section 3.2 (minimizing the F-norm formulation). For the divergence formulation of NMF, previous studies [16] successfully analyzed the convergence property of the multiplicative algorithm [27] from EM algorithm's maximum likelihood point of view. Such analysis is also valid in the GNMF case.

When $\lambda = 0$, it is easy to check that the updating rules in (20) and (21) reduce to the updating rules of the original NMF.

3.5 Computational Complexity Analysis

In this subsection, we discuss the extra computational cost of our proposed algorithm in comparison to standard NMF. Specifically, we provide the computational complexity analysis of GNMF for both F-Norm and KL-Divergence formulations.

The common way to express the complexity of one algorithm is using big O notation [10]. However, this is not precise enough to differentiate between the complexities of GNMF and NMF. Thus, we count the arithmetic operations for each algorithm.

Based on the updating rules, it is not hard to count the arithmetic operations of each iteration in NMF. We summarize the result in Table 1. For GNMF, it is important to note that \mathbf{W} is a sparse matrix. If we use a p -nearest neighbor graph, the average nonzero elements on each row of \mathbf{W} is p . Thus, we only need NpK flam (a floating-point addition and multiplication) to compute \mathbf{WV} . We also summarize the arithmetic operations for GNMF in Table 1.

The updating rule (Eq. 21) in GNMF with the divergence formulation involves inverting a large matrix $\sum_i u_{ik} \mathbf{I} + \lambda \mathbf{L}$. In reality, there is no need to actually compute the inversion. We only need to solve the linear equations system as follows:

$$\left(\sum_i u_{ik} \mathbf{I} + \lambda \mathbf{L} \right) \mathbf{v}_k = \begin{bmatrix} v_{1k} \sum_i \left(x_{i1}u_{ik} / \sum_k u_{ik}v_{1k} \right) \\ v_{2k} \sum_i \left(x_{i2}u_{ik} / \sum_k u_{ik}v_{2k} \right) \\ \vdots \\ v_{Nk} \sum_i \left(x_{iN}u_{ik} / \sum_k u_{ik}v_{Nk} \right) \end{bmatrix}$$

TABLE 1
Computational operation counts for each iteration in NMF and GNMF

| | F-norm formulation | | | |
|------|----------------------------------|---|------------------|-----------------------|
| | fladd | flmlt | fldiv | overall |
| NMF | $2MNK + 2(M + N)K^2$ | $2MNK + 2(M + N)K^2 + (M + N)K$ | $(M + N)K$ | $O(MNK)$ |
| GNMF | $2MNK + 2(M + N)K^2 + N(p + 3)K$ | $2MNK + 2(M + N)K^2 + (M + N)K + N(p + 1)K$ | $(M + N)K$ | $O(MNK)$ |
| | Divergence formulation | | | |
| | fladd | flmlt | fldiv | overall |
| NMF | $4MNK + (M + N)K$ | $4MNK + (M + N)K$ | $2MN + (M + N)K$ | $O(MNK)$ |
| GNMF | $4MNK + (M + 2N)K + q(p + 4)NK$ | $4MNK + (M + N)K + Np + q(p + 4)NK$ | $2MN + MK$ | $O((M + q(p + 4))NK)$ |

fladd: a floating-point addition
 N : the number of sample points
 p : the number of nearest neighbors
 flmlt: a floating-point multiplication
 M : the number of features
 q : the number of iterations in CG
 fldiv: a floating-point division
 K : the number of factors

Since matrix $\sum_i u_{ik} \mathbf{I} + \lambda \mathbf{L}$ is symmetric, positive-definite and sparse, we can use the iterative algorithm Conjugate Gradient (CG) [20] to solve this linear system of equations very efficiently. In each iteration, CG needs to compute the matrix-vector products in the form of $(\sum_i u_{ik} \mathbf{I} + \lambda \mathbf{L})\mathbf{p}$. The remaining work load of CG in each iteration is $4N$ flam. Thus, the time cost of CG in each iteration is $pN + 4N$. If CG stops after q iterations, the total time cost is $q(p + 4)N$. CG converges very fast, usually within 20 iterations. Since we need to solve K linear equations systems, the total time cost is $q(p + 4)NK$.

Besides the multiplicative updates, GNMF also needs $O(N^2M)$ to construct the p -nearest neighbor graph. Suppose the multiplicative updates stops after t iterations, the overall cost for NMF (both formulations) is

$$O(tMNK). \quad (22)$$

The overall cost for GNMF with F-norm formulation is

$$O(tMNK + N^2M) \quad (23)$$

and the cost for GNMF with divergence formulation is

$$O(t(M + q(p + 4))NK + N^2M). \quad (24)$$

4 EXPERIMENTAL RESULTS

Previous studies show that NMF is very powerful for clustering, especially in the document clustering and image clustering tasks [42], [37]. It can achieve similar or better performance than most of the state-of-the-art clustering algorithms, including the popular spectral clustering methods [32], [42].

Assume that a document corpus is comprised of K clusters each of which corresponds to a coherent topic. To accurately cluster the given document corpus, it is ideal to project the documents into a K -dimensional semantic space in which each axis corresponds to a particular topic [42]. In this semantic space, each document can be represented as a linear combination of the K topics. Because it is more natural to consider each document as an additive rather than a subtractive mixture of the underlying topics, the combination coefficients should all take non-negative values [42]. These

TABLE 2
Statistics of the three data sets

| dataset | size (N) | dimensionality (M) | # of classes (K) |
|---------|--------------|------------------------|----------------------|
| COIL20 | 1440 | 1024 | 20 |
| PIE | 2856 | 1024 | 68 |
| TDT2 | 9394 | 36771 | 30 |

values can be used to decide the cluster membership. In appearance-based visual analysis, an image may be also associated with some hidden parts. For example, a face image can be thought of as a combination of nose, mouth, eyes, etc. It is also reasonable to require the combination coefficients to be non-negative. This is the main motivation of applying NMF on document and image clustering. In this section, we also evaluate our GNMF algorithm on document and image clustering problems.

For the purpose of reproducibility, we provide the code and data sets at:

<http://www.zjucadcg.cn/dengcai/Data/GNMF.html>

4.1 Data Sets

Three data sets are used in the experiment. Two of them are image data sets and the third one is a document corpus. The important statistics of these data sets are summarized below (see also Table 2):

- The first data set is COIL20 image library, which contains 32×32 gray scale images of 20 objects viewed from varying angles.
- The second data set is the CMU PIE face database, which contains 32×32 gray scale face images of 68 persons. Each person has 42 facial images under different light and illumination conditions.
- The third data set is the NIST Topic Detection and Tracking (TDT2) corpus. The TDT2 corpus consists of data collected during the first half of 1998 and taken from 6 sources, including 2 newswires (APW, NYT), 2 radio programs (VOA, PRI) and 2 television programs (CNN, ABC). It consists of 11201 on-topic documents which are classified into 96 semantic categories. In this experiment, those documents appearing in two or more categories were removed,

TABLE 3
Clustering performance on COIL20

| K | Accuracy (%) | | | | | Normalized Mutual Information (%) | | | | |
|------|--------------|-----------|-----------|-----------|------------------|-----------------------------------|-----------|-----------|-----------|------------------|
| | Kmeans | PCA | NCut | NMF | GNMF | Kmeans | PCA | NCut | NMF | GNMF |
| 4 | 83.0±15.2 | 83.1±15.0 | 89.4±11.1 | 81.0±14.2 | 93.5±10.1 | 74.6±18.3 | 74.4±18.2 | 83.4±15.1 | 71.8±18.4 | 90.9±12.7 |
| 6 | 74.5±10.3 | 75.5±12.2 | 83.6±11.3 | 74.3±10.1 | 92.4±6.1 | 73.2±11.4 | 73.1±12.1 | 80.9±11.6 | 71.9±11.6 | 91.1±5.6 |
| 8 | 68.6±5.7 | 70.4±9.3 | 79.1±7.7 | 69.3±8.6 | 84.0±9.6 | 71.8±6.8 | 72.8±8.3 | 79.1±6.6 | 71.0±7.4 | 89.0±6.5 |
| 10 | 69.6±8.0 | 70.8±7.2 | 79.4±7.6 | 69.4±7.6 | 84.4±4.9 | 75.0±6.2 | 75.1±5.2 | 81.3±6.0 | 73.9±5.7 | 89.2±3.3 |
| 12 | 65.0±6.8 | 64.3±4.6 | 74.9±5.5 | 69.0±6.3 | 81.0±8.3 | 73.1±5.6 | 72.5±4.6 | 78.6±5.1 | 73.3±5.5 | 88.0±4.9 |
| 14 | 64.0±4.9 | 67.3±6.2 | 71.5±5.6 | 67.6±5.6 | 79.2±5.2 | 73.3±4.2 | 74.9±4.9 | 78.1±3.8 | 73.8±4.6 | 87.3±3.0 |
| 16 | 64.0±4.9 | 64.1±4.9 | 70.7±4.1 | 66.0±6.0 | 76.8±4.1 | 74.6±3.1 | 74.5±2.7 | 78.0±2.8 | 73.4±4.2 | 86.5±2.0 |
| 18 | 62.7±4.7 | 62.3±4.3 | 67.2±4.1 | 62.8±3.7 | 76.0±3.0 | 73.7±2.6 | 73.9±2.5 | 76.3±3.0 | 72.4±2.4 | 85.8±1.8 |
| 20 | 63.7 | 64.3 | 69.6 | 60.5 | 75.3 | 73.4 | 74.5 | 77.0 | 72.5 | 87.5 |
| Avg. | 68.3 | 69.1 | 76.2 | 68.9 | 82.5 | 73.6 | 74.0 | 79.2 | 72.7 | 88.4 |

TABLE 4
Clustering performance on PIE

| K | Accuracy (%) | | | | | Normalized Mutual Information (%) | | | | |
|-----|--------------|----------|-----------------|----------|-----------------|-----------------------------------|----------|-----------------|----------|-----------------|
| | Kmeans | PCA | NCut | NMF | GNMF | Kmeans | PCA | NCut | NMF | GNMF |
| 10 | 29.0±3.7 | 29.8±3.3 | 82.5±8.6 | 57.8±6.3 | 80.3±8.7 | 34.8±4.1 | 35.8±3.9 | 88.0±5.2 | 66.2±4.0 | 86.1±5.5 |
| 20 | 27.9±2.2 | 27.7±2.4 | 75.9±4.4 | 62.0±3.5 | 79.5±5.2 | 44.9±2.4 | 44.7±2.8 | 84.8±2.4 | 77.2±1.7 | 88.0±2.8 |
| 30 | 26.1±1.3 | 26.5±1.7 | 74.4±3.6 | 63.3±3.7 | 78.9±4.5 | 48.4±1.8 | 48.8±1.5 | 84.3±1.2 | 80.4±1.1 | 89.1±1.6 |
| 40 | 25.4±1.4 | 25.6±1.6 | 70.4±2.9 | 63.7±2.4 | 77.1±3.2 | 50.9±1.7 | 50.9±1.8 | 82.3±1.2 | 82.0±1.1 | 88.6±1.2 |
| 50 | 25.0±0.8 | 24.6±1.0 | 68.2±2.2 | 65.2±2.9 | 75.7±3.0 | 52.6±0.8 | 51.9±1.3 | 81.6±1.0 | 83.4±0.9 | 88.8±1.1 |
| 60 | 24.2±0.8 | 24.6±0.7 | 67.7±2.1 | 65.1±1.4 | 74.6±2.7 | 53.0±1.0 | 53.4±0.9 | 80.9±0.6 | 84.1±0.5 | 88.7±0.9 |
| 68 | 23.9 | 25.0 | 65.9 | 66.2 | 75.4 | 55.1 | 54.7 | 80.3 | 85.8 | 88.6 |
| Avg | 25.9 | 26.3 | 73.6 | 63.3 | 77.4 | 48.5 | 48.6 | 83.6 | 79.9 | 88.3 |

TABLE 5
Clustering performance on TDT2

| K | Accuracy (%) | | | | | Normalized Mutual Information (%) | | | | |
|------|--------------|-----------|-----------|-----------|-----------------|-----------------------------------|-----------|-----------|-----------|-----------------|
| | Kmeans | SVD | NCut | NMF | GNMF | Kmeans | SVD | NCut | NMF | GNMF |
| 5 | 80.8±17.5 | 82.7±16.0 | 96.4±0.7 | 95.5±10.2 | 98.5±2.8 | 78.1±19.0 | 76.8±20.3 | 93.1±3.9 | 92.7±14.0 | 94.2±8.9 |
| 10 | 68.5±15.3 | 68.2±13.6 | 88.2±10.8 | 83.6±12.2 | 91.4±7.6 | 73.1±13.5 | 69.2±14.0 | 83.4±11.1 | 82.4±11.9 | 85.6±9.2 |
| 15 | 64.9±8.7 | 65.3±7.2 | 82.1±11.2 | 79.9±11.7 | 93.4±2.7 | 74.0±7.9 | 71.8±8.9 | 81.1±9.8 | 82.0±9.2 | 88.0±5.7 |
| 20 | 63.9±4.2 | 63.4±5.5 | 79.0±8.1 | 76.3±5.6 | 91.2±2.6 | 75.7±4.5 | 71.5±5.6 | 78.9±6.3 | 80.6±4.5 | 85.9±4.1 |
| 25 | 61.5±4.3 | 60.8±4.0 | 74.3±4.8 | 75.0±4.5 | 88.6±2.1 | 74.6±2.4 | 70.9±2.3 | 77.1±2.7 | 79.0±2.5 | 83.9±2.6 |
| 30 | 61.2 | 65.9 | 71.2 | 71.9 | 88.6 | 74.7 | 74.7 | 76.5 | 77.4 | 83.7 |
| Avg. | 66.8 | 67.7 | 81.9 | 80.4 | 92.0 | 75.0 | 72.5 | 81.7 | 82.4 | 86.9 |

and only the largest 30 categories were kept, thus leaving us with 9,394 documents in total.

4.2 Compared Algorithms

To demonstrate how the clustering performance can be improved by our method, we compare the following five popular clustering algorithms:

- Canonical Kmeans clustering method (Kmeans in short).
- Kmeans clustering in the Principle Component subspace (PCA in short). Principle Component Analysis (PCA) [24] is one of the most well known unsupervised dimensionality reduction algorithms. It is expected that the cluster structure will be more explicit in the principle component subspace. Mathematically, PCA is equivalent to performing SVD on the centered data matrix. On the TDT2 data set, we simply use SVD instead of PCA because the centered data matrix is too large to be fit into memory. Actually, SVD has been very successfully used for document representation (*Latent Semantic Indexing*,

[11]). Interestingly, Zha *et al.* [44] has shown that Kmeans clustering in the SVD subspace has a close connection to Average Association [38], which is a popular spectral clustering algorithm. They showed that if the inner product is used to measure the similarity and construct the graph, Kmeans after SVD is equivalent to average association.

- Normalized Cut [38], one of the typical spectral clustering algorithms (NCut in short).
- Nonnegative Matrix Factorization based clustering (NMF in short). We use the F-norm formulation and implement a normalized cut weighted version of NMF as suggested in [42]. We provide a brief description of normalized cut weighted version of NMF and GNMF in Appendix C. Please refer to [42] for more details.
- Graph regularized Nonnegative Matrix Factorization (GNMF in short) with F-norm formulation, which is the new algorithm proposed in this paper. We use the 0-1 weighting scheme for constructing the p -nearest neighbor graph for its simplicity. The number of nearest neighbors p is set to 5 and

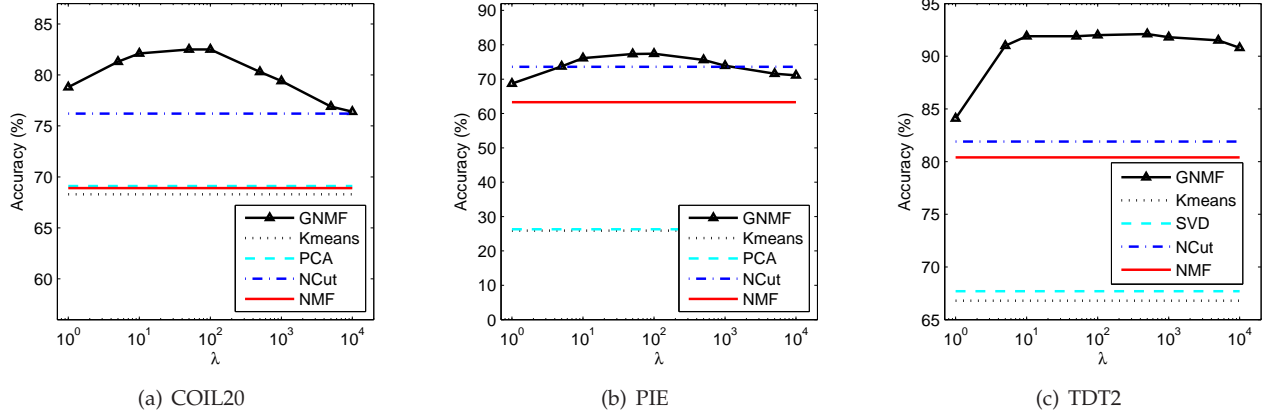


Fig. 1. The performance of GNMf vs. parameter λ . The GNMf is stable with respect to the parameter λ . It achieves consistently good performance when λ varies from 10 to 1000.

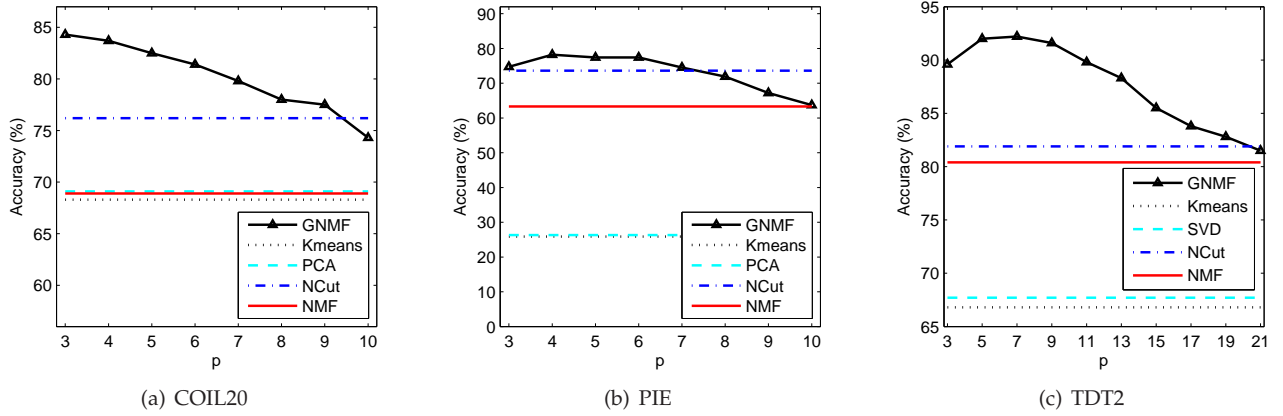


Fig. 2. The performance of GNMf decreases as the p increases.

the regularization parameter λ is set to 100. The parameter selection and weighting scheme selection will be discussed in the later section.

Among these five algorithms, NMF and GNMf can learn a parts-based representation because they allow only additive, not subtractive, combinations. NCut and GNMf are the two approaches which consider the intrinsic geometrical structure of the data.

The clustering result is evaluated by comparing the obtained label of each sample with the label provided by the data set. Two metrics, the accuracy (AC) and the normalized mutual information metric (NMI) are used to measure the clustering performance. Please see [4] for the detailed definitions of these two metrics.

4.3 Clustering Results

Tables 3, 4 and 5 show the clustering results on the COIL20, PIE and TDT2 data sets, respectively. In order to randomize the experiments, we conduct the evaluations with different cluster numbers. For each given cluster number K , 20 test runs were conducted on different randomly chosen clusters (except the case when the entire data set is used). The mean and standard error of the performance are reported in the tables.

These experiments reveal a number of interesting points:

- The non-negative matrix factorization based methods, both NMF and GNMf, outperform the PCA (SVD) method, which suggests the superiority of parts-based representation idea in discovering the hidden factors.
- Both NCut and GNMf consider the geometrical structure of the data and achieve better performance than the other three algorithms. This suggests the importance of the geometrical structure in learning the hidden factors.
- Regardless of the data sets, our GNMf always results in the best performance. This shows that by leveraging the power of both the parts-based representation and graph Laplacian regularization, GNMf can learn a better compact representation.

4.4 Parameters Selection

Our GNMf model has two essential parameters: the number of nearest neighbors p and the regularization parameter λ . Figure 1 and Figure 2 show how the average performance of GNMf varies with the parameters λ and p , respectively.

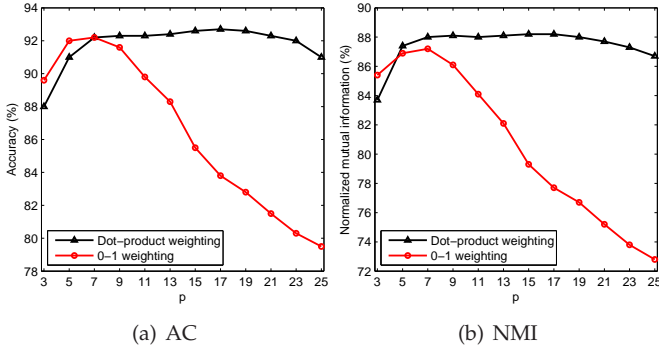


Fig. 3. The performance of GNMF vs. the parameter λ with different weighting schemes (dot-product vs. 0-1 weighting) on TDT2 data set.

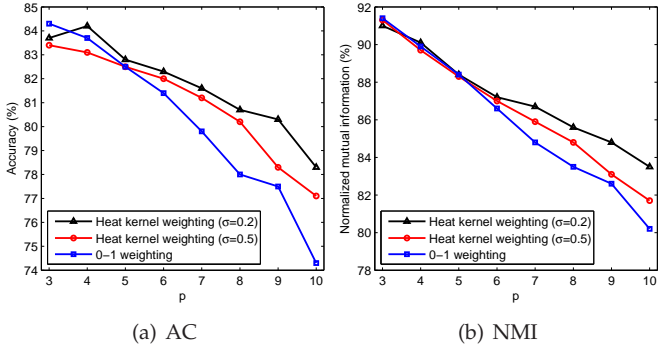


Fig. 4. The performance of GNMF vs. the parameter λ with different weighting schemes (heat kernel vs. 0-1 weighting) on COIL20 data set.

As we can see, the performance of GNMF is very stable with respect to the parameter λ . GNMF achieves consistently good performance when λ varies from 10 to 1000 on all three data sets.

As we have described, GNMF uses a p -nearest graph to capture the local geometric structure of the data distribution. The success of GNMF relies on the assumption that two neighboring data points share the same label. Obviously this assumption is more likely to fail as p increases. This is the reason why the performance of GNMF decreases as p increases, as shown in Figure 2.

4.5 Weighting Scheme Selection

There are many choices on how to define the weight matrix \mathbf{W} on the p -nearest neighbor graph. Three most popular ones are 0-1 weighting, heat kernel weighting and dot-product weighting. In our previous experiment, we use 0-1 weighting for its simplicity. Given a point \mathbf{x} , 0-1 weighting treats its p nearest neighbors equally important. However in many cases, it is necessary to differentiate these p neighbors, especially when p is large. In this case, one can use heat kernel weighting or dot-product weighting.

For text analysis tasks, the document vectors usually have been normalized to unit. In this case, the dot-

product of two document vectors becomes their cosine similarity, which is a widely used similarity measure for document in information retrieval community. Thus, it is very natural to use dot-product weighting for text data. Similar to 0-1 weighting, there is also no parameter for dot-product weighting. Figure 3 shows the performance of GNMF as a function of the number of nearest neighbors p for both dot-product and 0-1 weighting schemes on TDT2 data set. It is clear that dot-product weighting performs better than 0-1 weighting, especially when p is large. For dot-product weighting, the performance of GNMF remains reasonably good as p increases to 23. Whereas the performance of GNMF decreases dramatically for 0-1 weighting as p increases (when larger than 9).

For image data, a reasonable weighting scheme is heat kernel weighting. Figure 4 shows the performance of GNMF as a function of the number of nearest neighbors p for heat kernel and 0-1 weighting schemes on COIL20 data set. We can see that heat kernel weighting is also superior than 0-1 weighting, especially when p is large. However, there is a parameter σ in heat kernel weighting which is very crucial to the performance. Automatically selecting σ in heat kernel weighting is a challenging problem and has received a lot of interest in recent studies. A more detailed analysis of this subject is beyond the scope of this paper. Interested readers can refer to [43] for more details.

4.6 Convergence Study

The updating rules for minimizing the objective function of GNMF are essentially iterative. We have proved that these rules are convergent. Here we investigate how fast these rules can converge.

Figure 5 shows the convergence curves of both NMF and GNMF on all the three data sets. For each figure, the y-axis is the value of objective function and the x-axis denotes the iteration number. We can see that the multiplicative update rules for both GNMF and NMF converge very fast, usually within 100 iterations.

4.7 Sparseness Study

NMF only allows additive combinations between the basis vectors and it is believed that this property enables NMF to learn a *parts-based* representation [26]. Recent studies show that NMF does not always result in parts-based representations [22], [23]. Several researchers addressed this problem by incorporating the sparseness constraints on \mathbf{U} and/or \mathbf{V} [23]. In this subsection, we investigate the sparseness of the basis vectors learned in GNMF.

Figure 6 and 7 shows the basis vectors learned by NMF and GNMF in the COIL20 and PIE data sets respectively. Each basis vector has dimensionality 1024 and has unit norm. We plot these basis vectors as 32×32 gray scale images. It is clear to see that the basis vectors learned by GNMF are sparser than those learned by

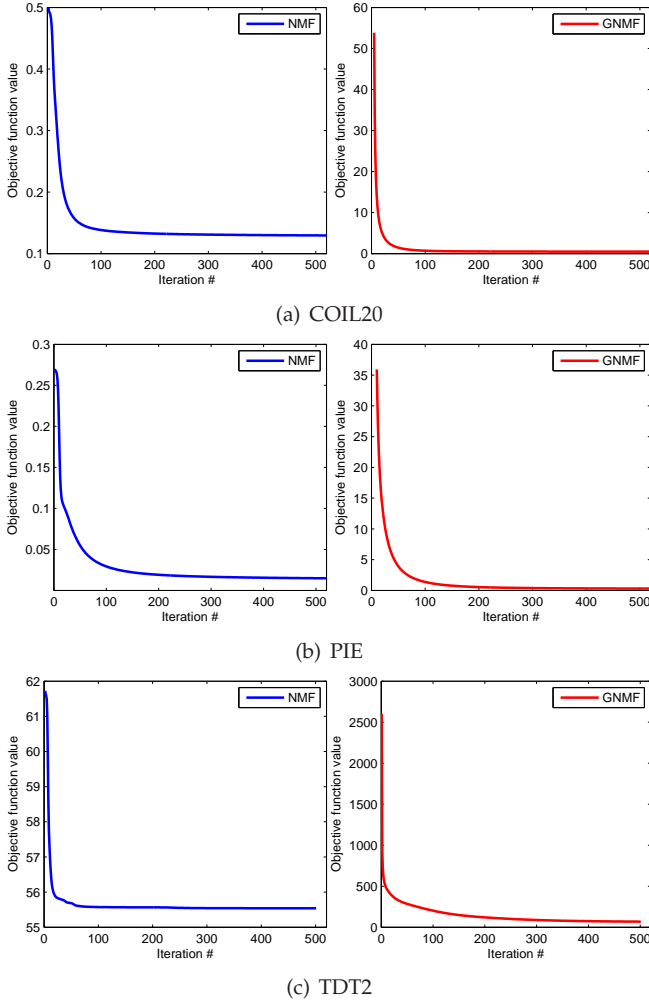


Fig. 5. Convergence curve of NMF and GNMF

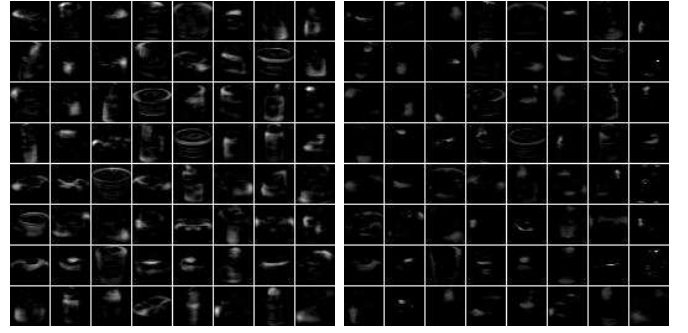
NMF. This result suggests that GNMF can learn a better *parts-based* representation than NMF.

5 CONCLUSIONS AND FUTURE WORK

We have presented a novel method for matrix factorization, called Graph regularized Non-negative Matrix Factorization (GNMF). GNMF models the data space as a submanifold embedded in the ambient space and performs the non-negative matrix factorization on this manifold. As a result, GNMF can have more discriminating power than the ordinary NMF approach which only considers the Euclidean structure of the data. Experimental results on document and image clustering show that GNMF provides a better representation in the sense of semantic structure.

Several questions remain to be investigated in our future work:

- 1) There is a parameter λ which controls the smoothness of our GNMF model. GNMF boils down to original NMF when $\lambda = 0$. Thus, a suitable value of λ is critical to our algorithm. It remains unclear how to do model selection theoretically and efficiently.



(a) Basis vectors (column vectors of U) learned by NMF (b) Basis vectors (column vectors of U) learned by GNMF

Fig. 6. Basis vectors learned from the COIL20 data set.



(a) Basis vectors (column vectors of U) learned by NMF (b) Basis vectors (column vectors of U) learned by GNMF

Fig. 7. Basis vectors learned from the PIE data set.

- 2) NMF is an optimization of convex cone structure [14]. Instead of preserving the locality of close points in a Euclidean manner, preserving the locality of angle similarity might fit more to the NMF framework. This suggests another way to extend NMF.
- 3) Our convergence proofs essentially follows the idea in the proofs of Lee and Seung's paper [27] for the original NMF. For the F-norm formulation, Lin [30] shows that Lee and Seung's multiplicative algorithm cannot guarantee the convergence to a stationary point and suggests minor modifications on Lee and Seung's algorithm which can converge. Our updating rules in Eq. (14) and (15) are essentially similar to the updating rules for NMF. It is interesting to apply Lin's idea to GNMF approach.

ACKNOWLEDGMENTS

This work was supported in part by National Natural Science Foundation of China under Grants 60905001 and 90920303, National Key Basic Research Foundation of China under Grant 2009CB320801, NSF IIS-09-05215 and the U.S. Army Research Laboratory under Cooperative Agreement Number W911NF-09-2-0053 (NS-CTA). Any opinions, findings, and conclusions expressed here are those of the authors and do not necessarily reflect the views of the funding agencies.

APPENDIX A (PROOFS OF THEOREM 1):

The objective function \mathcal{O}_1 of GNMF in Eq. (6) is certainly bounded from below by zero. To prove Theorem 1, we need to show that \mathcal{O}_1 is non-increasing under the updating steps in Eq. (14) and (15). Since the second term of \mathcal{O}_1 is only related to \mathbf{V} , we have exactly the same update formula for \mathbf{U} in GNMF as in the original NMF. Thus, we can use the convergence proof of NMF to show that \mathcal{O}_1 is nonincreasing under the update step in Eq. (14). Please see [27] for details.

Now we only need to prove that \mathcal{O}_1 is non-increasing under the updating step in Eq. (15). We will follow the similar procedure described in [27]. Our proof will make use of an auxiliary function similar to that used in the Expectation-Maximization algorithm [12]. We begin with the definition of the *auxiliary function*.

Definition $G(v, v')$ is an *auxiliary function* for $F(v)$ if the conditions

$$G(v, v') \geq F(v), \quad G(v, v) = F(v)$$

are satisfied.

The auxiliary function is very useful because of the following lemma.

Lemma 3: If G is an auxiliary function of F , then F is non-increasing under the update

$$v^{(t+1)} = \arg \min_v G(v, v^{(t)}) \quad (25)$$

Proof:

$$F(v^{(t+1)}) \leq G(v^{(t+1)}, v^{(t)}) \leq G(v^{(t)}, v^{(t)}) = F(v^{(t)})$$

■

□

Now we will show that the update step for \mathbf{V} in Eq. (15) is exactly the update in Eq. (25) with a proper auxiliary function.

We rewrite the objective function \mathcal{O}_1 of GNMF in Eq. (6) as follows

$$\begin{aligned} \mathcal{O}_1 &= \|\mathbf{X} - \mathbf{U}\mathbf{V}^T\|^2 + \lambda \text{Tr}(\mathbf{V}^T \mathbf{L} \mathbf{V}) \\ &= \sum_{i=1}^M \sum_{j=1}^N (x_{ij} - \sum_{k=1}^K u_{ik} v_{jk})^2 + \lambda \sum_{k=1}^K \sum_{j=1}^N \sum_{l=1}^N v_{jk} L_{jl} v_{lk} \end{aligned} \quad (26)$$

Considering any element v_{ab} in \mathbf{V} , we use F_{ab} to denote the part of \mathcal{O}_1 which is only relevant to v_{ab} . It is easy to check that

$$F'_{ab} = \left(\frac{\partial \mathcal{O}_1}{\partial \mathbf{V}} \right)_{ab} = \left(-2\mathbf{X}^T \mathbf{U} + 2\mathbf{V} \mathbf{U}^T \mathbf{U} + 2\lambda \mathbf{L} \mathbf{V} \right)_{ab} \quad (27)$$

$$F''_{ab} = 2(\mathbf{U}^T \mathbf{U})_{bb} + 2\lambda \mathbf{L}_{aa} \quad (28)$$

Since our update is essentially element-wise, it is sufficient to show that each F_{ab} is nonincreasing under the update step of Eq. (15).

Lemma 4: Function

$$\begin{aligned} G(v, v_{ab}^{(t)}) &= F_{ab}(v_{ab}^{(t)}) + F'_{ab}(v_{ab}^{(t)})(v - v_{ab}^{(t)}) \\ &\quad + \frac{(\mathbf{V} \mathbf{U}^T \mathbf{U})_{ab} + \lambda(\mathbf{D} \mathbf{V})_{ab}}{v_{ab}^{(t)}} (v - v_{ab}^{(t)})^2 \end{aligned} \quad (29)$$

is an auxiliary function for F_{ab} , the part of \mathcal{O}_1 which is only relevant to v_{ab} .

Proof: Since $G(v, v) = F_{ab}(v)$ is obvious, we need only show that $G(v, v_{ab}^{(t)}) \geq F_{ab}(v)$. To do this, we compare the Taylor series expansion of $F_{ab}(v)$

$$\begin{aligned} F_{ab}(v) &= F_{ab}(v_{ab}^{(t)}) + F'_{ab}(v_{ab}^{(t)})(v - v_{ab}^{(t)}) \\ &\quad + \frac{1}{2}[(\mathbf{U}^T \mathbf{U})_{bb} + \lambda \mathbf{L}_{aa}](v - v_{ab}^{(t)})^2 \end{aligned} \quad (30)$$

with Eq. (29) to find that $G(v, v_{ab}^{(t)}) \geq F_{ab}(v)$ is equivalent to

$$\frac{(\mathbf{V} \mathbf{U}^T \mathbf{U})_{ab} + \lambda(\mathbf{D} \mathbf{V})_{ab}}{v_{ab}^{(t)}} \geq (\mathbf{U}^T \mathbf{U})_{bb} + \lambda \mathbf{L}_{aa}. \quad (31)$$

We have

$$(\mathbf{V} \mathbf{U}^T \mathbf{U})_{ab} = \sum_{l=1}^k v_{al}^{(t)} (\mathbf{U}^T \mathbf{U})_{lb} \geq v_{ab}^{(t)} (\mathbf{U}^T \mathbf{U})_{bb} \quad (32)$$

and

$$\begin{aligned} \lambda(\mathbf{D} \mathbf{V})_{ab} &= \lambda \sum_{j=1}^M \mathbf{D}_{aj} v_{jb}^{(t)} \geq \lambda \mathbf{D}_{aa} v_{ab}^{(t)} \\ &\geq \lambda(\mathbf{D} - \mathbf{W})_{aa} v_{ab}^{(t)} = \lambda \mathbf{L}_{aa} v_{ab}^{(t)} \end{aligned} \quad (33)$$

Thus, Eq. (31) holds and $G(v, v_{ab}^{(t)}) \geq F_{ab}(v)$. ■

□

We can now demonstrate the convergence of Theorem 1:

Proof of Theorem 1: Replacing $G(v, v_{ab}^{(t)})$ in Eq. (25) by Eq. (29) results in the update rule:

$$\begin{aligned} v_{ab}^{(t+1)} &= v_{ab}^{(t)} - v_{ab}^{(t)} \frac{F'_{ab}(v_{ab}^{(t)})}{2(\mathbf{V} \mathbf{U}^T \mathbf{U})_{ab} + 2\lambda(\mathbf{D} \mathbf{V})_{ab}} \\ &= v_{ab}^{(t)} \frac{(\mathbf{X}^T \mathbf{U} + \lambda \mathbf{W} \mathbf{V})_{ab}}{(\mathbf{V} \mathbf{U}^T \mathbf{U} + \lambda \mathbf{D} \mathbf{V})_{ab}} \end{aligned} \quad (34)$$

Since Eq. (29) is an auxiliary function, F_{ab} is nonincreasing under this update rule. ■

APPENDIX B (PROOFS OF THEOREM 2):

Similarly, the second term of \mathcal{O}_2 in Eq. (7) is only related to \mathbf{V} , we have exactly the same update formula for \mathbf{U} in GNMF as the original NMF. Thus, we can use the convergence proof of NMF to show that \mathcal{O}_2 is nonincreasing under the update step in Eq. (20). Please see [27] for details.

Now we will show that the update step for \mathbf{V} in Eq. (21) is exactly the update in Eq. (25) with a proper auxiliary function.

Lemma 5: Function

$$G(\mathbf{V}, \mathbf{V}^{(t)})$$

$$\begin{aligned} &= \sum_{i,j} \left(x_{ij} \log x_{ij} - x_{ij} + \sum_{k=1}^K u_{ik} v_{jk} \right) \\ &\quad - \sum_{i,j,k} \left(x_{ij} \frac{u_{ik} v_{jk}^{(t)}}{\sum_k u_{ik} v_{jk}^{(t)}} \left(\log u_{ik} v_{jk} - \log \frac{u_{ik} v_{jk}^{(t)}}{\sum_k u_{ik} v_{jk}^{(t)}} \right) \right) \\ &\quad + \frac{\lambda}{2} \sum_{j,l,k} \left(v_{jk} \log \frac{v_{jk}}{v_{lk}} + v_{lk} \log \frac{v_{lk}}{v_{jk}} \right) \mathbf{W}_{jl} \end{aligned}$$

is an auxiliary function for the objective function of GNMF in Eq. (7)

$$\begin{aligned} F(\mathbf{V}) &= \sum_{i,j} \left(x_{ij} \log \frac{x_{ij}}{\sum_k u_{ik} v_{jk}} - x_{ij} + \sum_k u_{ik} v_{jk} \right) \\ &\quad + \frac{\lambda}{2} \sum_{j,l,k} \left(v_{jk} \log \frac{v_{jk}}{v_{lk}} + v_{lk} \log \frac{v_{lk}}{v_{jk}} \right) \mathbf{W}_{jl} \end{aligned}$$

Proof: It is straightforward to verify that $G(\mathbf{V}, \mathbf{V}) = F(\mathbf{V})$. To show that $G(\mathbf{V}, \mathbf{V}^{(t)}) \geq F(\mathbf{V})$, we use convexity of the log function to derive the inequality

$$-\log \left(\sum_{k=1}^K u_{ik} v_{jk} \right) \leq -\sum_{k=1}^K \left(\alpha_k \log \frac{u_{ik} v_{jk}}{\alpha_k} \right)$$

which holds for all nonnegative α_k that sum to unity. Setting

$$\alpha_k = \frac{u_{ik} v_{jk}^{(t)}}{\sum_{k=1}^K u_{ik} v_{jk}^{(t)}},$$

we obtain

$$\begin{aligned} &-\log \left(\sum_k u_{ik} v_{jk} \right) \leq \\ &-\sum_k \left(\frac{u_{ik} v_{jk}^{(t)}}{\sum_k u_{ik} v_{jk}^{(t)}} \left(\log u_{ik} v_{jk} - \log \frac{u_{ik} v_{jk}^{(t)}}{\sum_k u_{ik} v_{jk}^{(t)}} \right) \right). \end{aligned}$$

From this inequality it follows that $G(\mathbf{V}, \mathbf{V}^{(t)}) \geq F(\mathbf{V})$. \square

Theorem 2 then follows from the application of Lemma 5:

Proof of Theorem 2: The minimum of $G(\mathbf{V}, \mathbf{V}^{(t)})$ with respect to \mathbf{V} is determined by setting the gradient to zero:

$$\begin{aligned} &\sum_{i=1}^M u_{ik} - \sum_{i=1}^M x_{ij} \frac{u_{ik} v_{jk}^{(t)}}{\sum_k u_{ik} v_{jk}^{(t)}} \frac{1}{v_{jk}} \\ &\quad + \frac{\lambda}{2} \sum_{l=1}^N \left(\log \frac{v_{jk}}{v_{lk}} + 1 - \frac{v_{lk}}{v_{jk}} \right) \mathbf{W}_{jl} = 0, \end{aligned} \quad (35)$$

$$1 \leq j \leq N, \quad 1 \leq k \leq K$$

Because of the log term, it is really hard to solve the above system of equations. Let us recall the motivation of the regularization term. We hope that if two data points \mathbf{x}_j and \mathbf{x}_r are close (i.e. \mathbf{W}_{jr} is big), \mathbf{z}_j will be close to \mathbf{z}_r

and v_{js}/v_{rs} will be approximately 1. Thus, we can use the following approximation:

$$\log(x) \approx 1 - \frac{1}{x}, \quad x \rightarrow 1.$$

The above approximation is based on the first order expansion of Taylor series of the log function. With this approximation, the equations in Eq. (35) can be written as

$$\begin{aligned} &\sum_{i=1}^M u_{ik} - \sum_{i=1}^M x_{ij} \frac{u_{ik} v_{jk}^{(t)}}{\sum_k u_{ik} v_{jk}^{(t)}} \frac{1}{v_{jk}} \\ &\quad + \frac{\lambda}{v_{jk}} \sum_{l=1}^N (v_{jk} - v_{lk}) \mathbf{W}_{jl} = 0, \end{aligned} \quad (36)$$

$$1 \leq j \leq N, \quad 1 \leq k \leq K$$

Let \mathbf{D} denote a diagonal matrix whose entries are column (or row, since \mathbf{W} is symmetric) sums of \mathbf{W} , $\mathbf{D}_{jj} = \sum_l \mathbf{W}_{jl}$. Define $\mathbf{L} = \mathbf{D} - \mathbf{W}$. Let \mathbf{v}_k denote the k -th column of \mathbf{V} , $\mathbf{v}_k = [v_{1k}, \dots, v_{Nk}]^T$. It is easy to verify that $\sum_l (v_{jl} - v_{lk}) \mathbf{W}_{jl}$ equals to the j -th element of vector $\mathbf{L}\mathbf{v}_k$.

The system of equations in Eq. (36) can be rewritten as

$$\sum_i u_{ik} \mathbf{I} \mathbf{v}_k + \lambda \mathbf{L} \mathbf{v}_k = \begin{bmatrix} v_{1k}^{(t)} \sum_i \left(x_{i1} u_{ik} / \sum_k u_{ik} v_{1k}^{(t)} \right) \\ \vdots \\ v_{Nk}^{(t)} \sum_i \left(x_{iN} u_{ik} / \sum_k u_{ik} v_{Nk}^{(t)} \right) \end{bmatrix},$$

$$1 \leq k \leq K.$$

Thus, the update rule of Eq. (25) takes the form

$$\mathbf{v}_k^{(t+1)} = \left(\sum_i u_{ik} \mathbf{I} + \lambda \mathbf{L} \right)^{-1} \begin{bmatrix} v_{1k}^{(t)} \sum_i \left(x_{i1} u_{ik} / \sum_k u_{ik} v_{1k}^{(t)} \right) \\ \vdots \\ v_{Nk}^{(t)} \sum_i \left(x_{iN} u_{ik} / \sum_k u_{ik} v_{Nk}^{(t)} \right) \end{bmatrix},$$

$$1 \leq k \leq K.$$

Since G is an auxiliary function, F is nonincreasing under this update. \blacksquare

APPENDIX C (WEIGHTED NMF AND GNMF)

In this appendix, we provide a brief description of normalized cut weighted NMF which is first introduced by Xu *et al.* [42]. Let \mathbf{z}_j^T be j -th row vector of \mathbf{V} , the objective function of NMF can be written as:

$$O = \sum_{j=1}^N (\mathbf{x}_j - \mathbf{U} \mathbf{z}_j)^T (\mathbf{x}_j - \mathbf{U} \mathbf{z}_j),$$

which is the summation of the reconstruction errors over all the data points, and each data point is equally weighted. If each data point has weight γ_j , the objective

function of weighted NMF can be written as:

$$\begin{aligned}
O' &= \sum_{j=1}^N \gamma_j (\mathbf{x}_j - \mathbf{Uz}_j)^T (\mathbf{x}_j - \mathbf{Uz}_j) \\
&= \text{Tr} \left((\mathbf{X} - \mathbf{UV}^T) \Gamma (\mathbf{X} - \mathbf{UV}^T)^T \right) \\
&= \text{Tr} \left((\mathbf{X}\Gamma^{1/2} - \mathbf{UV}^T \Gamma^{1/2}) (\mathbf{X}\Gamma^{1/2} - \mathbf{UV}^T \Gamma^{1/2})^T \right) \\
&= \text{Tr} \left((\mathbf{X}' - \mathbf{UV}'^T)^T (\mathbf{X}' - \mathbf{UV}'^T) \right)
\end{aligned}$$

where Γ is the diagonal matrix consists of γ_j , $\mathbf{V}' = \Gamma^{1/2} \mathbf{V}$ and $\mathbf{X}' = \mathbf{X}\Gamma^{1/2}$. Notice that the above equation has the same form as Eq. (1) in Section 2 (the objective function of NMF), so the same algorithm for NMF can be used to find the solution of this weighted NMF problem. In [42], Xu *et al.* calculate $\mathbf{D} = \text{diag}(\mathbf{X}^T \mathbf{X} \mathbf{e})$, where \mathbf{e} is a vector of all ones. They use \mathbf{D}^{-1} as the weight and named this approach as normalized cut weighted NMF (NMF-NCW). The experimental results [42] have demonstrated the effectiveness of this weighted approach on document clustering.

Similarly, we can also introduce this weighting scheme into our GNMF approach. The objective function of weighted GNMF is:

$$\begin{aligned}
O' &= \sum_{j=1}^N \gamma_j (\mathbf{x}_j - \mathbf{Uz}_j)^T (\mathbf{x}_j - \mathbf{Uz}_j) + \lambda \text{Tr}(\mathbf{V}^T \mathbf{L} \mathbf{V}) \\
&= \text{Tr} \left((\mathbf{X} - \mathbf{UV}^T) \Gamma (\mathbf{X} - \mathbf{UV}^T)^T \right) + \lambda \text{Tr}(\mathbf{V}^T \mathbf{L} \mathbf{V}) \\
&= \text{Tr} \left((\mathbf{X}\Gamma^{1/2} - \mathbf{UV}^T \Gamma^{1/2}) (\mathbf{X}\Gamma^{1/2} - \mathbf{UV}^T \Gamma^{1/2})^T \right) \\
&\quad + \lambda \text{Tr}(\mathbf{V}^T \mathbf{L} \mathbf{V}) \\
&= \text{Tr} \left((\mathbf{X}' - \mathbf{UV}'^T)^T (\mathbf{X}' - \mathbf{UV}'^T) \right) + \lambda \text{Tr}(\mathbf{V}'^T \mathbf{L}' \mathbf{V}')
\end{aligned}$$

where Γ , \mathbf{V}' , \mathbf{X}' are defined as before and $\mathbf{L}' = \Gamma^{-1/2} \mathbf{L} \Gamma^{-1/2}$. Notice that the above equation has the same form as Eq. (8) in Section 3.2, so the same algorithm for GNMF can be used to find the solution of weighted GNMF problem.

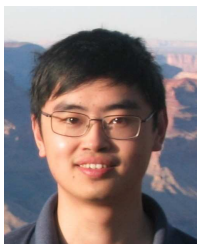
REFERENCES

- [1] M. Belkin and P. Niyogi. Laplacian eigenmaps and spectral techniques for embedding and clustering. In *Advances in Neural Information Processing Systems 14*, pages 585–591. MIT Press, Cambridge, MA, 2001. 1, 3
- [2] M. Belkin, P. Niyogi, and V. Sindhwani. Manifold regularization: A geometric framework for learning from examples. *Journal of Machine Learning Research*, 7:2399–2434, 2006. 1, 2, 3
- [3] J.-P. Brunet, P. Tamayo, T. R. Golub, and J. P. Mesirov. Meta-genes and molecular pattern discovery using matrix factorization. *Proceedings of the National Academy of Sciences*, 101(12):4164–4169, 2004. 3
- [4] D. Cai, X. He, and J. Han. Document clustering using locality preserving indexing. *IEEE Transactions on Knowledge and Data Engineering*, 17(12):1624–1637, December 2005. 8
- [5] D. Cai, X. He, X. Wang, H. Bao, and J. Han. Locality preserving nonnegative matrix factorization. In *Proc. 2009 Int. Joint Conference on Artificial Intelligence (IJCAI'09)*, 2009. 2
- [6] D. Cai, X. He, X. Wu, and J. Han. Non-negative matrix factorization on manifold. In *Proc. Int. Conf. on Data Mining (ICDM'08)*, 2008. 2
- [7] D. Cai, X. Wang, and X. He. Probabilistic dyadic data analysis with local and global consistency. In *Proceedings of the 26th Annual International Conference on Machine Learning (ICML'09)*, pages 105–112, 2009. 2, 3
- [8] M. Catral, L. Han, M. Neumann, and R. Plemmons. On reduced rank nonnegative matrix factorization for symmetric nonnegative matrices. *Linear Algebra and Its Applications*, 393:107–126, 2004. 4
- [9] F. R. K. Chung. *Spectral Graph Theory*, volume 92 of *Regional Conference Series in Mathematics*. AMS, 1997. 3, 4
- [10] T. H. Cormen, C. E. Leiserson, R. L. Rivest, and C. Stein. *Introduction to Algorithms*. MIT Press and McGraw-Hill, 2nd edition, 2001. 5
- [11] S. C. Deerwester, S. T. Dumais, T. K. Landauer, G. W. Furnas, and R. A. Harshman. Indexing by latent semantic analysis. *Journal of the American Society of Information Science*, 41(6):391–407, 1990. 1, 7
- [12] A. P. Dempster, N. M. Laird, and D. B. Rubin. Maximum likelihood from incomplete data via the em algorithm. *Journal of the Royal Statistical Society. Series B (Methodological)*, 39(1):1–38, 1977. 11
- [13] C. Ding, T. Li, and W. Peng. Nonnegative matrix factorization and probabilistic latent semantic indexing: Equivalence, chi-square statistic, and a hybrid method. In *Proc. 2006 AAAI Conf. on Artificial Intelligence (AAAI-06)*, 2006. 2
- [14] D. Donoho and V. Stodden. When does non-negative matrix factorization give a correct decomposition into parts? In *Advances in Neural Information Processing Systems 16*. MIT Press, Cambridge, MA, 2003. 10
- [15] R. O. Duda, P. E. Hart, and D. G. Stork. *Pattern Classification*. Wiley-Interscience, Hoboken, NJ, 2nd edition, 2000. 1
- [16] L. Finesso and P. Spreij. Nonnegative matrix factorization and i-divergence alternating minimization. *Linear Algebra and Its Applications*, 416(2-3):270–287, 2006. 5
- [17] E. Gaussier and C. Goutte. Relation between pls and nmf and implications. In *SIGIR '05: Proceedings of the 28th annual international ACM SIGIR conference on Research and development in information retrieval*, pages 601–602, 2005. 2
- [18] R. Hadsell, S. Chopra, and Y. LeCun. Dimensionality reduction by learning an invariant mapping. In *Proceedings of the 2006 IEEE Computer Society Conference on Computer Vision and Pattern Recognition (CVPR'06)*, pages 1735–1742, 2006. 1
- [19] X. He and P. Niyogi. Locality preserving projections. In *Advances in Neural Information Processing Systems 16*. MIT Press, Cambridge, MA, 2003. 3
- [20] M. R. Hestenes and E. Stiefel. Methods of conjugate gradients for solving linear systems. *Journal of Research of the National Bureau of Standards*, 49(6), 1952. 6
- [21] T. Hofmann. Unsupervised learning by probabilistic latent semantic analysis. *Machine Learning*, 42(1-2):177–196, 2001. 2
- [22] P. O. Hoyer. Non-negative sparse coding. In *Proc. IEEE Workshop on Neural Networks for Signal Processing*, pages 557–565, 2002. 9
- [23] P. O. Hoyer. Non-negative matrix factorization with sparseness constraints. *Journal of Machine Learning Research*, 5:1457–1469, 2004. 9
- [24] I. T. Jolliffe. *Principal Component Analysis*. Springer-Verlag, New York, 1989. 7
- [25] J. Kivinen and M. K. Warmuth. Additive versus exponentiated gradient updates for linear prediction. In *STOC '95: Proceedings of the twenty-seventh annual ACM symposium on Theory of computing*, pages 209–218, 1995. 5
- [26] D. D. Lee and H. S. Seung. Learning the parts of objects by non-negative matrix factorization. *Nature*, 401:788–791, 1999. 1, 2, 3, 9
- [27] D. D. Lee and H. S. Seung. Algorithms for non-negative matrix factorization. In *Advances in Neural Information Processing Systems 13*. 2001. 2, 3, 4, 5, 10, 11
- [28] J. M. Lee. *Introduction to Smooth Manifolds*. Springer-Verlag New York, 2002. 1
- [29] S. Z. Li, X. Hou, H. Zhang, and Q. Cheng. Learning spatially localized, parts-based representation. In *2001 IEEE Computer Society Conference on Computer Vision and Pattern Recognition (CVPR'01)*, pages 207–212, 2001. 1, 3
- [30] C.-J. Lin. On the convergence of multiplicative update algorithms for non-negative matrix factorization. *IEEE Transactions on Neural Networks*, 18(6):1589–1596, 2007. 4, 10
- [31] N. K. Logothetis and D. L. Sheinberg. Visual object recognition. *Annual Review of Neuroscience*, 19:577–621, 1996. 1
- [32] A. Y. Ng, M. Jordan, and Y. Weiss. On spectral clustering: Analysis and an algorithm. In *Advances in Neural Information Processing*

- Systems 14*, pages 849–856. MIT Press, Cambridge, MA, 2001. 6
- [33] P. Paatero and U. Tapper. Positive matrix factorization: A non-negative factor model with optimal utilization of error estimates of data values. *Environmetrics*, 5(2):111–126, 1994. 1, 2
- [34] S. E. Palmer. Hierarchical structure in perceptual representation. *Cognitive Psychology*, 9:441–474, 1977. 1
- [35] S. Roweis and L. Saul. Nonlinear dimensionality reduction by locally linear embedding. *Science*, 290(5500):2323–2326, 2000. 1
- [36] H. S. Seung and D. D. Lee. The manifold ways of perception. *Science*, 290(12), 2000. 1
- [37] F. Shahnaza, M. W. Berrya, V. Paucab, and R. J. Plemmons. Document clustering using nonnegative matrix factorization. *Information Processing & Management*, 42(2):373–386, 2006. 6
- [38] J. Shi and J. Malik. Normalized cuts and image segmentation. *IEEE Transactions on Pattern Analysis and Machine Intelligence*, 22(8):888–905, 2000. 7
- [39] J. Tenenbaum, V. de Silva, and J. Langford. A global geometric framework for nonlinear dimensionality reduction. *Science*, 290(5500):2319–2323, 2000. 1
- [40] M. Turk and A. Pentland. Eigenfaces for recognition. *Journal of Cognitive Neuroscience*, 3(1):71–86, 1991. 1
- [41] E. Wachsmuth, M. W. Oram, and D. I. Perrett. Recognition of objects and their component parts: Responses of single units in the temporal cortex of the macaque. *Cerebral Cortex*, 4:509–522, 1994. 1
- [42] W. Xu, X. Liu, and Y. Gong. Document clustering based on non-negative matrix factorization. In *Proc. 2003 Int. Conf. on Research and Development in Information Retrieval (SIGIR '03)*, pages 267–273, Toronto, Canada, Aug. 2003. 1, 3, 4, 6, 7, 12, 13
- [43] L. Zelnik-manor and P. Perona. Self-tuning spectral clustering. In *Advances in Neural Information Processing Systems 17*, pages 1601–1608. MIT Press, 2004. 9
- [44] H. Zha, C. Ding, M. Gu, X. He, and H. Simon. Spectral relaxation for k-means clustering. In *Advances in Neural Information Processing Systems 14*, pages 1057–1064. MIT Press, Cambridge, MA, 2001. 7
- [45] D. Zhou, O. Bousquet, T. Lal, J. Weston, and B. Schölkopf. Learning with local and global consistency. In *Advances in Neural Information Processing Systems 16*, 2003. 3
- [46] X. Zhu and J. Lafferty. Harmonic mixtures: combining mixture models and graph-based methods for inductive and scalable semi-supervised learning. In *ICML '05: Proceedings of the 22nd international conference on Machine learning*, pages 1052–1059, 2005. 3



Deng Cai is an Associate Professor in the State Key Lab of CAD&CG, College of Computer Science at Zhejiang University, China. He received the PhD degree in computer science from University of Illinois at Urbana Champaign in 2009. Before that, he received his Bachelor's degree and a Master's degree from Tsinghua University in 2000 and 2003 respectively, both in automation. His research interests include machine learning, data mining and information retrieval.



Xiaofei He received the BS degree in Computer Science from Zhejiang University, China, in 2000 and the Ph.D. degree in Computer Science from the University of Chicago, in 2005. He is a Professor in the State Key Lab of CAD&CG at Zhejiang University, China. Prior to joining Zhejiang University, he was a Research Scientist at Yahoo! Research Labs, Burbank, CA. His research interests include machine learning, information retrieval, and computer vision.



Jiawei Han is a Professor of Computer Science at the University of Illinois. He has chaired or served in over 100 program committees of the major international conferences in the fields of data mining and database systems, and also served or is serving on the editorial boards for *Data Mining and Knowledge Discovery*, *IEEE Transactions on Knowledge and Data Engineering*, *Journal of Computer Science and Technology*, and *Journal of Intelligent Information Systems*. He is the founding Editor-in-Chief of *ACM Transactions on Knowledge Discovery from Data (TKDD)*. Jiawei has received IBM Faculty Awards, HP Innovation Awards, ACM SIGKDD Innovation Award (2004), IEEE Computer Society Technical Achievement Award (2005), and IEEE W. Wallace McDowell Award (2009). He is a Fellow of ACM and IEEE. He is currently the Director of Information Network Academic Research Center (INARC) supported by the Network Science-Collaborative Technology Alliance (NS-CTA) program of U.S. Army Research Lab. His book "Data Mining: Concepts and Techniques" (Morgan Kaufmann) has been used worldwide as a textbook.



Thomas S. Huang received his Sc.D. from the Massachusetts Institute of Technology in Electrical Engineering, and was on the faculty of MIT and Purdue University. He joined University of Illinois at Urbana Champaign in 1980 and is currently William L. Everitt Distinguished Professor of Electrical and Computer Engineering, Research Professor of Coordinated Science Laboratory, Professor of the Center for Advanced Study, and Co-Chair of the Human Computer Intelligent Interaction major research theme of the Beckman Institute for Advanced Science and Technology. Huang is a member of the National Academy of Engineering and has received numerous honors and awards, including the IEEE Jack S. Kilby Signal Processing Medal (with Ar. Netravali) and the King-Sun Fu Prize of the International Association of Pattern Recognition. He has published 21 books and more than 600 technical papers in network theory, digital holography, image and video compression, multimodal human computer interfaces, and multimedia databases.